|| Volume 5 || Issue 2 || February 2020 || ISSN (Online) 2456-0774
INTERNATIONAL JOURNAL OF ADVANCE SCIENTIFIC RESEARCH
AND ENGINEERING TRENDS

NBO, HIRSHFELD SURFACE AND MESP STUDY OF N-(4-Aminobenzoyl) glycine

K.Rajalakshmi [1], M.Vetrivel[2]

Assistant Professor, Department of Physics, SCSVMV, Kanchipuram
Associate Professor, Department of Mechanical Engg., SCSVMV, Kanchipurnam
kr@kanchiuniv.ac.in

Abstract- In the present work, the optimized molecular geometry and harmonic vibrational frequencies of a derivative of hippuric acid were calculated by DFT/B3LYP method with 6-31+ G (d,p) basis set. Natural bond orbital analysis (NBO) has been performed on title compound using B3LYP/6-31 +G(d,p) levels in order to elucidate intermolecular hydrogen bonding, intermolecular charge transfer (ICT) and delocalization of electron density. The Hirshfeld surface analysis and 2D fingerprint plots were computed for the tile compound and reveal that the molecule have stabilized intermolecular interactions. Molecular Electrostatic Potential analysis (MESP) have been studied to predict compound reactivity.

Keywords: *N-(4-Aminobenzoyl) glycine; DFT; NBO; Hirshfeld surface; MESP*

I INTRODUCTION

N-(4-Aminobenzoyl) glycine is a derivative of hippuric acid that is formed from the combination of benzoic acid and glycine. The levels of this acid increases with the intake of phenol compounds such as fruit juice, tea and wine. These phenol compounds are first converted to benzoic acid and then to hippuric acid and then excreted in urine [1]. It is useful in the measurement of renal plasma flow, the volume of blood plasma delivered to the kidneys per unit time [2-4]. The glycine amide of 4-aminobenzoic acid. Its sodium salt is used as a diagnostic aid to measure effective renal plasma flow (ERPF) and to determine the functional capacity of the tubular excretory mechanism.

II COMPUTATIONAL DETAILS

All theoretical calculations were carried out with Gaussian 09 program package [5] using B3LYP [6-7] methods in conjunction with 6-31+ G(d,p) basis set. The molecular structure, MEP surfaces were visualized with Gauss View 5 program [8]. Natural Bond Orbital (NBO) calculations were performed using NBO 3.1 program [9] as implemented in the Gaussian 09 package at DFT/B3LYP levels. The second order Fock-matrix was carried out to evaluate the donor (i) and acceptor (j) interaction in the NBO basis [10]. For each donor (i) and acceptor (j), the stabilization energy $E^{(2)}$ is associated as:

$$E^{(2)} = E_{ij} = q_i \frac{F(i,j)^2}{(\varepsilon_i - \varepsilon_j)}$$

The larger the $E^{(2)}$ value, the more intensive is the interaction between electron donor and electron acceptor which means more donating tendency from electron donors to acceptors and a greater extent of conjugation of the whole system.

III RESULTS AND DISCUSSIONS

3.1 Molecular Geometry

The molecule has 24 atoms. A molecule consisting of N atoms has a total of 3N degrees of freedom, corresponding to the Cartesian coordinates of each atom in the molecule. In a nonlinear molecule, 3 of these degrees belong to the rotational, 3 of these degrees belong to the translational motions of the molecule and so the remaining corresponds to its vibrational motions. The net number of the vibrational modes is 3N-6. Therefore, for the title molecule, three Cartesian displacements of 24 atoms provide 66 normal vibration modes. The molecular structure of the molecule is shown in Fig.1.

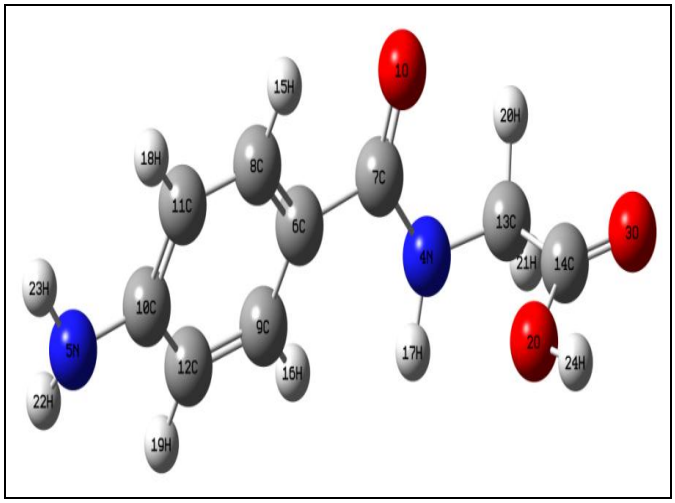

Figure 1 Molecular structure of the title compound

3.2 Natural Bonding Orbital analysis

Natural bonding orbital (NBO analysis) calculations were done with the help of NBO 3.1 program implemented in Gaussian 09 W Suite at DFT/B3LYP/6 -31+ G(d, p) level of theory and the second order interactions obtained by NBO analysis are listed in Table 1 and Table 2.

The important intermolecular hyper conjugative interactions are: C13-C14 from N4 of LP(N4) LP(N4) → σ*(C13-C14), O3-C14 from O2 of LP (O2) → σ*(O3-C14), C13-C14 from O2-H24 of σ (O2-H24) → σ* (C13-C14), C10-C12 from N5-H23 of σ (N5-H23) → σ* (C10-C14), C10-C12 from C11-H18 of σ (C11-H18) → σ* (C10-C12) with electron densities 0.07944, 0.02726, 0.0794 , 0.40669 and 0.02262e and stabilization energies 10.31, 8.09, 4.71,4.27 and 4.22 kJ/mol. Almost 100% p-character was observed at lone pairs of O2 (99.87) , O1 (99.76) O3 (99.71) and N4 (97.02) respectively [11].

Table 1: Second-order perturbation theory of Fock matrix in NBO basis corresponding to the intramolecular bonds of the title compound

Donor (i)	**Type**	**ED/e**	**Acceptor (j)**	**Type**	**ED/e**	**E(2)[a] (Kcal/mol)**	**E(j)- E(i)[b] (a.u)**	**F(i,j)[c] (a.u)**
O1-C7	σ	1.99349	C6-C7	σ*	0.06340	1.26	1.46	0.039
O1-C7	σ	1.99349	C6-C9	σ*	0.02272	1.42	1.58	0.042
O2-H24	σ	1.98674	O3-C14	σ*	0.02726	0.64	1.34	0.026
O2-H24	σ	1.98674	C13-C14	σ*	0.07944	4.71	1.11	0.066
N4-C13	σ	1.98883	O3-C14	σ*	0.02726	1.92	1.34	0.045
N4-C13	σ	1.98883	C6-C7	σ*	0.06340	2.44	1.20	0.049
N4-H17	σ	1.98225	O1-C7	σ*	0.02354	4.14	1.23	0.064
N4-H17	σ	1.98225	C13-H20	σ*	0.01360	1.81	1.10	0.040
N5-C10	σ	1.99316	C9-C12	σ*	0.01283	1.37	1.39	0.039
N5-H23	σ	1.98869	C10-C12	σ*	0.40669	4.27	1.21	0.064
C6-C7	σ	1.97522	N4-C13	σ*	0.01887	3.34	1.02	0.052
C6-C7	σ	1.97522	C8-C11	σ*	0.01198	2.31	1.25	0.048
C6-C8	σ	1.97279	C6-C9	σ*	0.02272	3.41	1.25	0.058
C6-C8	σ	1.97279	C9-H16	σ*	0.01299	2.63	1.15	0.049
C6-C8	σ	1.97279	C11-H18	σ*	0.01243	2.41	1.14	0.047
C6-C9	σ	1.97539	C6-C8	σ*	0.02028	3.37	1.26	0.058
C6-C9	σ	1.97539	C9-C12	σ*	0.01283	2.48	1.28	0.050
C8-C11	σ	1.97845	N5-C10	σ*	0.01732	3.98	1.14	0.060
C8-C11	σ	1.97845	C6-C7	σ*	0.06340	2.61	1.14	0.049
C8-H15	σ	1.97882	C6-C9	σ*	0.02272	4.54	1.08	0.062
C8-H15	σ	1.97882	C10-C11	σ*	0.02295	3.87	1.06	0.057
C9-C12	σ	1.97792	N5-C10	σ*	0.01732	3.96	1.15	0.060
C9-C12	σ	1.97792	C6-C7	σ*	0.06340	3.23	1.15	0.055
C9-H16	σ	1.97973	C6-C8	σ*	0.02028	4.11	1.10	0.060
C9-H16	σ	1.97973	C10-C12	σ*	0.02262	3.78	1.08	0.057
C10-C12	σ	1.97418	C9-C12	σ*	0.01283	2.35	1.28	0.049
C10-C12	σ	1.97418	C10-C11	σ*	0.02295	2.94	1.25	0.054
C11-H18	σ	1.98062	C6-C8	σ*	0.02028	3.68	1.09	0.057
C11-H18	σ	1.98062	C10-C12	σ*	0.02262	4.22	1.07	0.060
C12-H19	σ	1.98074	C6-C9	σ*	0.02272	3.77	1.09	0.057
C12-H19	σ	1.98074	C10-C11	σ*	0.02295	4.15	1.08	0.060
C13-C14	σ	1.97703	O2-H24	σ*	0.01458	3.12	1.08	0.052
C13-H20	σ	1.96607	N4-H17	σ*	0.01826	3.80	0.96	0.054
LP O1	σ	1.97687	N4-C7	σ*	0.07566	1.48	1.13	0.037
LP O1	σ	1.97687	C6-C7	σ*	0.06340	2.37	1.12	0.047

LP O2	σ	1.97567	O3-C14	σ*	0.02726	8.09	1.20	0.088
LP O3	σ	1.97611	O2-C14	σ*	0.10289	1.76	1.05	0.039
LP O3	σ	1.97611	C13-C14	σ*	0.07944	2.35	1.06	0.045
LP N4	σ	1.73936	O1-C7	σ*	0.02354	2.10	0.83	0.040
LP N4	σ	1.73936	O3-C14	σ*	0.02726	0.51	0.85	0.020
LP N4	σ	1.73936	C13-C14	σ*	0.07944	10.31	0.62	0.075
LP N4	σ	1.73936	C13-H20	σ*	0.01360	0.58	0.71	0.019
LP N4	σ	1.73936	C13-H21	σ*	0.01170	2.12	0.69	0.036
LP N5	σ	1.82730	C10-C12	π*	0.02262	30.43	0.31	0.093

a $E^{(2)}$ means energy of hyper conjugative interaction (stabilization energy).

b Energy difference between donor and acceptor i and j NBO orbitals.

c F(i,j) is the Fock matrix element between i and j NBO orbitals.

Table 2 :NBO results showing the formation of Lewis and non-Lewis orbitals

Bond(A-B)	ED/e	EDA%	EDB%	NBO	s%	p%
σ (O1-C7)	1.99349	64.75	35.25	$0.8047(sp^{1.58})O$	38.55	61.07
-	-1.01911			$0.5937(sp^{2.21})C$	31.17	68.74
σ (O2-C14)	1.99633	68.35	31.65	$0.8268(sp^{2.01})O$	33.23	66.68
-	-0.38553			$0.5626((sp^{2.62})C$	27.55	72.21
σ (N4-C7)	1.98967	62.5	37.48	$0.7907(sp^{1.81})N$	35.61	64.36
	-0.81694			$0.6122(sp^{2.24})C$	30.82	69.05
σ (N5-C10)	1.99316	59.39	40.61	$0.7707(sp^{1.71})N$	36.84	63.12
	-0.81857			$0.6372(sp^{2.47})C$	28.77	71.13
σ (N5-H23)	1.99869	71.23	28.77	$0.8440(sp^{2.63})N$	27.51	72.44
	-0.66428			$0.5363(sp^{0.00})H$	99.89	0.11
σ (C8-C11)	1.97845	49.66	50.34	$0.7047(sp^{1.81})C$	35.51	64.45
	-0.70590			$0.7095(sp^{1.76})C$	36.18	63.78
σ (C9-H16)	1.97973	62.07	37.93	$0.7878(sp^{2.39})C$	29.47	70.49
	-0.53737			$0.6159(sp^{0.00})H$	99.95	0.05
σ (C12-H19)	1.98074	62.11	37.89	$0.7881(sp^{2.33})C$	30.05	69.91
	-0.53401			$0.6156(sp^{0.00})H$	99.95	0.05
σ (C13-C14)	1.97703	50.76	49.24	$0.7124(sp^{2.97})C$	25.20	74.74
	-0.66042			$0.7017(sp^{1.63})C$	37.98	61.97
σ LP O1	1.97687	-	-	$sp^{0.67}$	59.98	39.96
	-0.68530			-	-	-
π LP O1	1.86846	-	-	$sp^{1.00}$	0.00	99.76
	-0.24744			-	-	-
σ LP O2	1.97567	-	-	$sp^{1.26}$	44.26	55.68
	-0.63068			-	-	-
π LP O2	1.81849	-	-	$sp^{1.00}$	0.01	99.87
	-0.35220			-	-	-
σ LP O3	1.97611	-	-	$sp^{0.68}$	59.48	40.45
	-0.71472			-	-	-
π LP O3	1.84414	-	-	$sp^{1.00}$	0.01	99.71
	-0.27762			-	-	-
σ LP N4	1.73936	-	-	$sp^{32.76}$	2.96	97.02
	-0.27331			-	-	-
σ LPN5	1.82730	-	-	$sp^{11.43}$	8.04	91.92
	-0.29912			-	-	-

3.3 Hirshfeld surfaces computational method

3D-Hirshfeld surfaces [12-13] associated with 2D finger print analysis [14-15] was performed using a powerful graphical tool Crystal Explorer 3.1 suite [16] which accept CIF as the Input File. The 3D Hirshfeld surfaces and 2D finger print plots of the present investigated compound is depicted in Fig.2 and Fig.3. The surfaces of the title compound have been mapped over (a) d_{norm}, (b) shape index (c) and curvedness in the range of -0.7298 (red) to 1.2660 (blue), -1.0 (concave) to 1.0 Å au (convex) and -4.0 (flat) to 0.4 Å au (singular) respectively as shown in Fig.2 (a), Fig.2 (b) and Fig.2 (c). in d_{norm} surface, strong hydrogen bonds and nitrogen atoms result in bright red spots near the hydrogen bonding acceptor and donor atoms while the other interactions result in faint red spots. The d_{norm} mapped surfaces of the present compound exhibit interaction between the oxygen atom and the hydrogen atom can be visualized as bright red spots and the bond distances are shown in Fig.3.

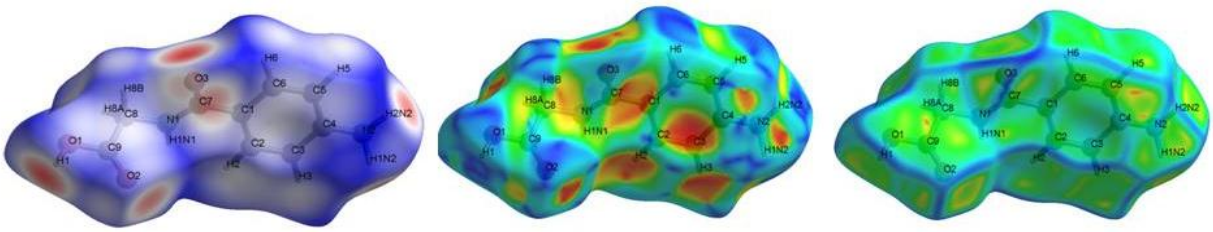

Fig. 2(a) Fig. 2(b) Fig. 2(c)

Fig.2(a) Hirshfeld surfaces of title compound d_{norm} -0.7298 (red) to 1.2660 Å au. (blue)
Fig.2 (b) shape index -1.0 (concave) to 1.0 Å au (convex)
Fig.2 (c) curvedness -4.0(flat) to 0.4 Å au (singular)

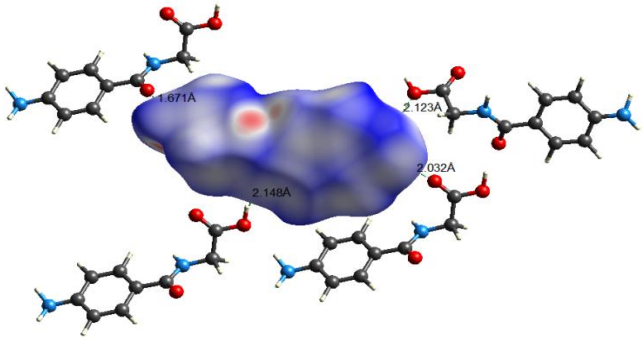

Figure 3 View of O...H contacts of d_{norm} surface of the title compound

From the decomposition of fingerprint plots of the investigated compound represents the major contributor's contacts on the surface of Hirshfeld namely H....H, O....H and C...H contacts. The intermolecular hydrogen bonds contacts H...H have the greatest contribution to the surface of Hirshfeld (35.9%) represented by two surfaces in the two dimensional fingerprint maps. The O...H contacts contribute to the surface of Hirshfeld (18.5%) represented by two sharp spikes in two dimensional fingerprint maps shown in Fig.4 (a), while the C...H contacts contribute to the surface of Hirshfeld (11.9%) represented by two sharp spikes in two dimensional fingerprint maps shown in Fig.4(b), and the N-H contacts contribute to the surface of Hirshfeld (2.3%) as shown in Fig.4(c) respectively. The relative contribution of the different interactions to the Hirshfeld surface is H...H, O...H and C...H interactions have major participations in crystal structures [17] .

It is clear from the Figure 4, that the interaction between O...H (18.5%) is observed in the form of spike with d_i value the distance from the surface to the nearest nucleus internal to the surface [O] is 1.2 Å au and au shown as red pointer marks in Fig.4(d) and d_e surface is the distance from the surface to the nearest nucleus external to the surface [H] is 0.5 Å au. Similarly, the interaction between C...H (11.9%) is observed in the form of spike with d_i value,the distance from the surface to the nearest nucleus internal to the surface [C] is 1.6 Å au shown as red pointer marks in Fig.4(e) and d_e surface is the distance from the surface to the nearest nucleus external to the surface [H] is 1.1 Å au and the interaction between N...H (2.3%) is observed in the form of spike with d_i value, the distance from the surface to the nearest nucleus internal to the surface [N] is 1.8 Å au and d_e surface is the distance from the surface to the nearest nucleus external to the surface [H] is 1.4 Å au shown as red pointer marks in

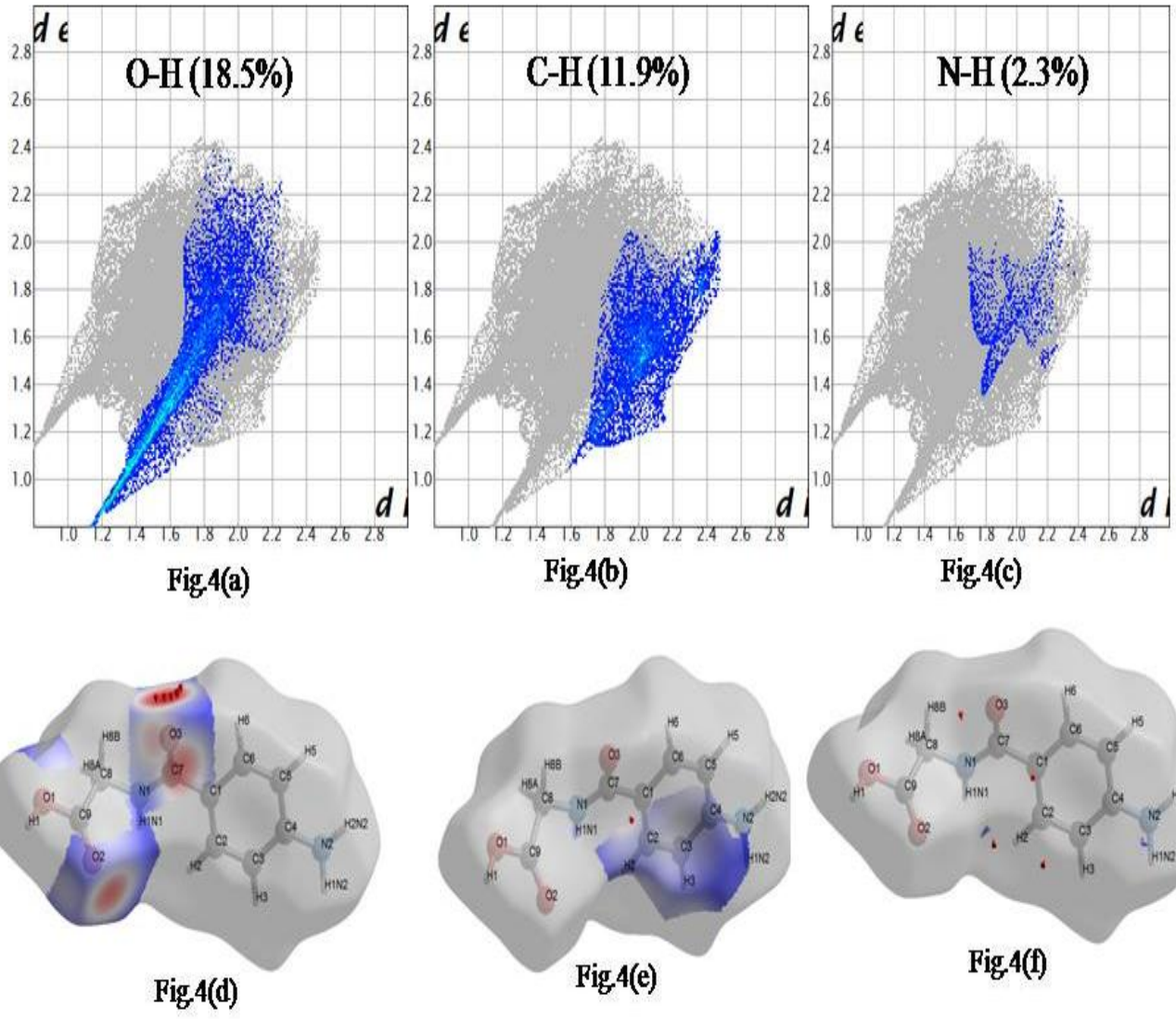

Figure 4 2D Fingerprints plots of title compound and various interactions are visualized with percentage of contact.

3.4 Molecular electrostatic potential Analysis

A useful tool in the analysis of chemical activity of molecules and their physiochemical properties is molecular electrostatic potential surface (MEP). From molecular electrostatic potential analysis, it is possible to obtain knowledge about interaction between molecules and biological particles, such as protein and enzymes [18]. The different colours on MEP surface represent different values of the electrostatic potential. The potential increases from the least to the most negative according to the following order: blue<green<yellow<red [19-20]. The total electron density was calculate for the isovalue density of 0.0004.

To investigate reactive sites for electrophilic and nucleophilic attack, the regions of the MEP for the title compound was composed at DFT calculation using the optimized geometry at the B3LYP/6-31+ G(d). It is clear from Fig.5, red and yellow colors indicate negative regions in MEP corresponding to electrophilic reactivity, while bluish green colors indicate for positive regions corresponding to nucleophilic reactivity. So, the compound has one major possible site for electrophilic attack.

In the investigated compound, the main areas of negative electrostatic potential are localized on oxygen (O1) and nitrogen atoms. The region of two potential minima is observed on the carbonyl group at C7-O1 position. The second area of potential minima is observed at hydroxyl group O2-H24 position and Carbonyl group of C4-O3 position. According to the calculated results, the region of MEP indicates that the negative molecular electrostatic potential on oxygen atoms indicating the major possible site for electrophilic attack and positive potential sites are around carbon and hydrogen atoms. The determination of MESP regions is best suitable for identifying sites for inter and intra molecular interactions.

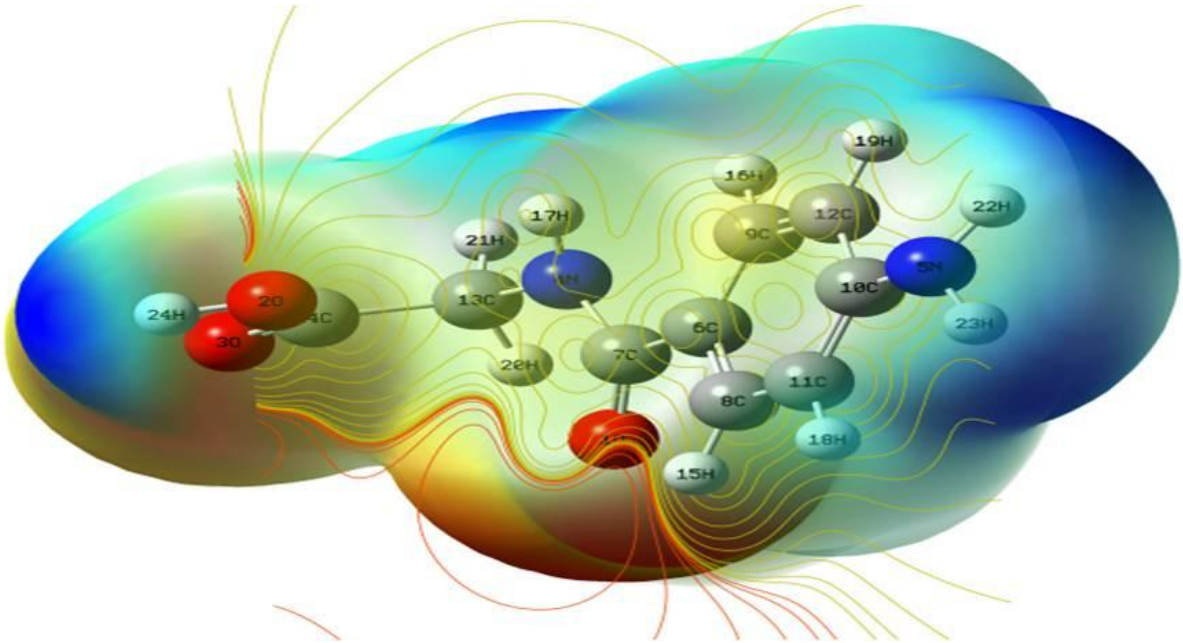

Figure 5. Colour-coded graphic representation of electrostatic potential map of the title compound.

IV CONCLUSION

Density functional calculations have been successfully performed for the title compound N-(4-Aminobenzoyl)glycine. The stability of the molecule arising from hyper-conjugative interaction and charge delocalization has been analyzed using NBO analysis. In this compound, NBO analysis reveals that a strong intramolecular hyper conjugative interaction of σ *-electrons with the large energy contributions from LP(N4) σ*(C13-C14), and LP (O2) σ*(O3-C14), have energy value of 10.31 and 8.09 kcal/mol. Also, 100% p-character was observed as lone pairs of O2,(99.87) , O1 (99.76) O3 (99.71) and N4 (97.02) respectively. The 3D Hirshfeld surfaces and 2D finger print plots of the present compound shows interaction between the oxygen and hydrogen atoms and contribution of the different interactions is due to H...H, O...H and C...H interactions in crystal structures. It has been found that the main areas of negative electrostatic potential are localized near the oxygen atoms and nitrogen atoms and the region of potential minima is observed on the on the carbonyl group at C7-O1 position and at hydroxyl group O2-H24 position.

REFERENCES

1. "Human Metabolome Database: Showing metabocard for Hippuric acid (HMDB0000714)". www.hmdb.ca. Retrieved 2018-09-21.
2. Costanzo, Linda. Physiology, 4th Edition. Philadelphia: Lippincott Williams and Wilkins, 2007; 156-160.
3. Reubi, François C. (1953-04-29). "Glomerular filtration rate, renal blood flow and blood viscosity during and after diabetic coma". Circ. Res. 1 (5): 410–3.
4. Beyer, Karl H, Flippin, Harrison, Verwey, W. F. Woodward, Roland (1944-12-16). "The Effect of Para-Aminohippuric Acid On Plasma Concentration Of Penicillin In Man". Journal of the American Medical Association. 126 (16): 1007–1009. doi:10.1001/jama.1944.02850510015003. ISSN 0002-9955.
5. Frisch MJ, et al., Gaussian 09, Revision B.01, Gaussian Inc., Wallingford CT2009.
6. Becke AD. Density-functional thermochemistry. III. The role of exact exchange. The Journal of Chemical Physics 1993; 98(7):5648-5652.
7. Lee C, Yang W , Parr RG. Development of the Colle-Salvetti correlation energy formula into a functional of the electron density. Physical Review B, 1988; 37 (2): 785-789.
8. Frisch E, Hratchian HP, Dennington II RD, Keith TA, Millam J, Nielsen B, Holder AJ, Hiscocks J. Gaussian, Inc. GaussView Version 5.0.8, Wallinford, CT. 2009.
9. Glendening ED, Reed AE, Carpenter JE & Weinhold F.NBO Version3.1, TCI, University of Wisconsin, Madison. 1998.

10. Foster JP, Weinhold F. Natural hybrid orbitals. Journal of the American Chemical Society, 1980;102(24): 7211-7218.
11. Rajalakshmi K. Gunasekaran S., Kumaresan S. Vibrational assignment, HOMO–LUMO and NBO analysis of (2S)-2-[(2-{[(2S)-1-hydroxybutan-2-yl]amino}ethyl)amino]butan-1-ol by density functional theory, Spectrochim.Acta Part A: 2014;130:466–479.
12. Spackman M.A., Jayatilaka D. Hirshfeld surface analysis, CrystEngComm 2009; 11: 19-32.
13. Hirshfeld F.L. Bonded-atom fragments for describing molecular charge densities, Theor. Chim. Acta 1977;44:129-138.
14. Rohl A.L., Moret M., Kaminsky W., Claborn K., McKinnon J.J., Kahr B. Hirshfeld surfaces identify inadequacies in computations of intermolecular interactions in crystals: pentamorphic 1,8-dihydroxyanthraquinone, Cryst. Growth Des. 2008; 8: 4517-4525.
15. Parkin A., Barr G., Dong W., Gilmore C.J., Jayatilaka D., McKinnon J.J. Spackman M.A., Wilson C.C. Comparing entire crystal structures: structural genetic fingerprinting, CrystEng Comm. 2007; 9: 648-652.
16. Wolff S.K., Grimwood D.J., McKinnon J.J., Jayatilaka D., Spackman M.A. Crystal Explorer 2.0, University of Western Australia, Australia, 2012.
17. Shyamapada Shit, Christoph Marschner,, Samiran Mitra. Synthesis, Crystal structure, and Hirshfeld Surface Analysis of a New Mixed Ligand Copper (II) Complex, Acta Chim. Slov. 2016;129 (63):, 129–137. DOI: 10.17344/acsi.2015.2024.
18. War J., Jalaja K., Mary Y., Panicker C., Armaković S., Armaković S., Srivastava S., Alsenoy C. Spectroscopic characterization of 1-[3-(1H-imidazol-1-yl)propyl]-3-phen- ylthiourea and assessment of reactive and optoelectronic properties employing DFT calculations and molecular dynamics simulations, J. Mol. Struct. 2017;1129:72–85,
19. Govindasamy P., Gunasekaran S., Quantum mechanical calculations and spectro- scopic (FT-IR, FT-Raman and UV) investigations, molecular orbital, NLO, NBO, NLMO and MESP analysis of 4-[5-(4-methylphenyl)-3-(trifluoromethyl)-1H- pyrazol-1-yl]benzene-1-sulfonamide, J. Mol. Struct. 2015; 1081:96–109.
20. Chandrasekaran K., Kumar R. Structural, spectral, thermodynamical, NLO, HOMO, LUMO and NBO analysis of fluconazole, Spectrochim. Acta A 2015; 150:974–991.